ELSEVIER

Polymer 41 (2000) 6895–6905

polymer

Nano-indentation of polymer–glass interfaces Part I. Experimental and mechanical analysis

A. Hodzic[a,*], Z.H. Stachurski[a], J.K. Kim[b]

[a]*Department of Engineering, The Australian National University ACT 0200 Canberra, Australia*
[b]*Department of Mechanical Engineering, The Hong Kong University of Science and Technology, Clear Water Bay, Kowloon, Hong Kong, People's Republic of China*

Received 22 September 1999; accepted 8 December 1999

Abstract

The interface region in polymer/glass composite materials was investigated by means of the nano-indentation and the nano-scratch techniques. The nano-indentation test involved indentations as small as 30 nm in depth in order to detect the material properties in the transition region between the fibre and the matrix. A line of nano indents was produced along the 14 μm path starting from the matrix and ending on the fibre. The distinct properties of the transition zone were revealed by 2–3 indents. The nano-scratch test involves moving a sample while being in contact with a diamond tip. The coefficient of friction, defined as the ratio of the tangential force from the tip–sample contact to the normal force, also indicated a transition zone of different width. Analysis of the results allowed elimination of effects due to: (i) indenter width and its geometry; (ii) stress field and plastic zone interactions, to arrive at true interphase width as a material characteristic. These two techniques proved to be useful tools in the investigation of the size and the character of the interphase region in the fibrous polymer/glass composite materials.

Keywords: Microindentation; Microhardness; Composite interface

1. Introduction

The interface is a sharp boundary between two materials in physical contact. By contrast, the interphase is defined as a region, which is formed because of bonding and reactions between the fibre and the matrix. The morphological features, chemical compositions and thermo-mechanical properties of the interphase, are distinct from the bulk materials [1]. Designed to enhance the bond between fibres and matrix in polymer/glass composite materials, silane coupling agents [2] react to varying degrees with different matrix polymers extending interphase regions deeper in the matrix. It is not yet clearly understood how the matrix properties are affected in the interphase region, where the silane physically and chemically interacts with the matrix polymer. The standard bulk testing of composite materials has shown that the bulk material properties have been improved with the presence of silane [3]. In order to understand better the interfacial mechanisms in composite materials and the role of coupling agents, several experimental techniques have been designed and employed to test local regions in the composite materials. Single fibre tests have been developed to minimise the influence of complicated stress transfer mechanisms in composites and to observe a test specimen containing a single bond [4]. Very important measurements have been carried out by means of Raman spectroscopy where it was observed that the stress distribution at the interface was far from linear and dependent on a surface treatment of the fibres [5,6]. Other experimental techniques such as Fourier transform infrared spectroscopy and NMR spectroscopy have been focussed on the chemical aspects of the interphase region [7–9], and finite element modelling [10]. Although providing important and otherwise unavailable information on the local characteristics in the composite materials, these tests could not provide the information on the material properties of the interphase region. Recently, the nano-indentation and the nano-scratch tests, originally designed to investigate the material properties of thin films and surfaces, have been employed in this direction [11,12]. In the work reported here, and previously [13], the nano-indentation tests were employed in order to investigate the material properties of the interphase region in phenolic/glass and polyester/glass systems. The nano-scratch test was used in conjuction with the nano-indentation test, in order to detect the total width of

* Corresponding author. Fax: + 612-6249-0506.
E-mail address: alma.hodzic@faceng.anu.edu.au (A. Hodzic).

0032-3861/00/$ - see front matter
PII: S0032-3861(99)00890-3

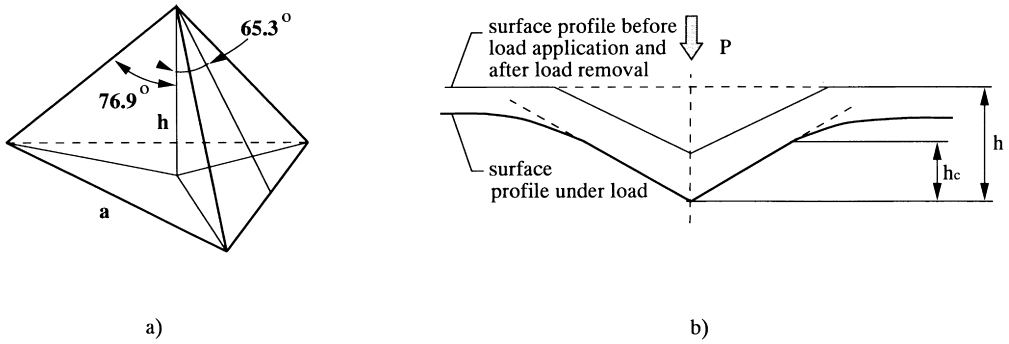

Fig. 1. (a) Shape and characteristic angles of the Berkovitch indenter. (b) Definition of depths (dimensions exaggerated for the sake of clarity).

the interphase region. In predicting the mechanical behaviour, important parts of a composite material are regions with different material properties. Hence, the nano-indentation and the nano-scratch techniques are an important step toward a better understanding of the multi-phase materials.

2. Experimental

2.1. Preparation of test materials

Three composite panels were made using:

1. phenolic resin Resinox CL1916 mixed with 7 wt% AH1964F hardener;
2. phenolic resin Resinox CL1880 mixed with 7 wt% H1196 hardener; and
3. polyester resin Synolite 0288-T-1 mixed with 2.4 wt% methyl ethyl ketone peroxide as a catalyst.

The fibres were unidirectional 450 g/m^2 E-type glass, 20 μm in diameter. The panels were made and supplied by the Aeronautical and Maritime Research Laboratory (AMRL) in Melbourne. One cube was cut from each composite material using a diamond saw. Dimensions of the cubes were $10 \times 5 \times 5$ mm. The surface of each cube in direction perpendicular to unidirectional glass fibres, consisted of perfectly cross-sectioned glass circles embedded in resin. The polishing process involved wet 600 and 800 Emery paper followed by 0.3 μm and finally 0.05 μm wet polishing alumina pastes.

2.2. Nano-indentation test

The apparatus used in this work was Nano Indenter II made by Nano Instruments, Inc. A detailed description of the instrument is available elsewhere [14]. The major components are the mobile indenter head, an optical microscope attached to a video camera and a sample holder rigidly fixed to an x–y–z motorised table. A sample prepared for

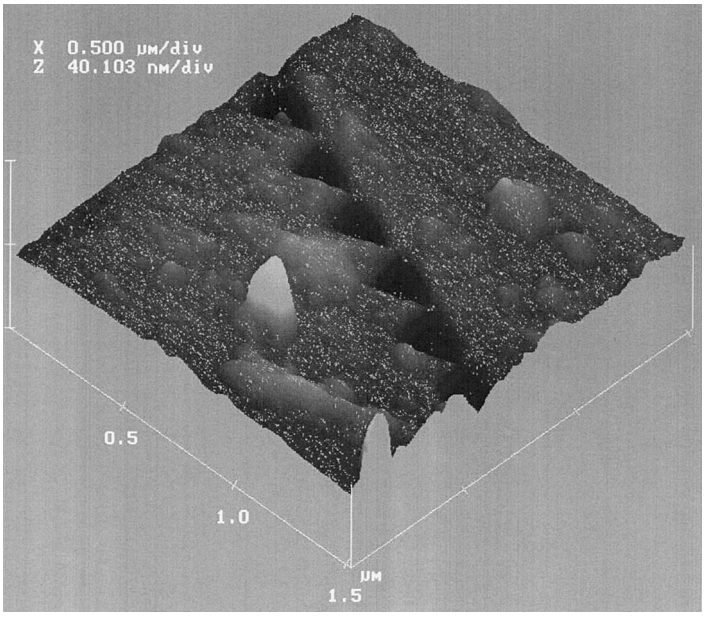

Fig. 2. AFM image of the glass fibre surface with a line of indents. Vertical scale is 40 nm per division.

testing is mounted in the sample holder and positioned by the motorised precision table, visually controlled through the optical microscope. The Berkovich indenter, mounted on the indenter head, is a three-sided triangular-based pyramidal diamond with a geometry as shown in Fig. 1. This type of indenter is commonly used for measurements of mechanical properties on the nano scale. Due to its well-defined geometry, it is capable of making well-defined indentation impressions [14]. Depths of indents were programmed to have a constant value of 30 nm. Displacements of indentation depths were consistent with +10 nm tolerance. From the shape of the Berkovich indenter (Fig. 1), the resulting indents were 210 nm wide. Each successive indent was displaced by 260 nm in order to avoid overlapping of plastic deformation zone onto neighbouring indents. The indents were made along a path of 7 μm in the matrix and 7 μm in the fibre, a total length of approximately 14 μm. A part of the line of indents in glass fibre is shown in Fig. 2. The image of the surface after the nano-indentation experiment was produced by Atomic Force Microscope operated in contact mode (Multi Mode Scanning Probe Microscope with Nano Scope E controller, by Digital Instrument). Since the depths of indents had a constant value, the load required to produce an indent was higher for harder material. Because loads of indents are sensitive to differences in depths, hardness is used instead as a more reliable value for comparison of data. Hardness of material calculated from an indent produced by Berkovich tip is calculated from the equation below:

$$H = \frac{P}{24.5h_c^2} \tag{1}$$

where: P is the load and h_c is the contact depth of the indent, as shown in Fig. 1.

2.3. Nano-scratch test

The nano-scratch test involves moving a sample while being in contact with the diamond tip. The indenter tip is replaced by the scratch tip with the same geometry but oriented with the sharp edge into the direction of motion. The normal force is maintained at a constant value and the lateral force is measured from the deflection of the shaft and the lateral displacement. The ratio of these two forces is the coefficient of friction between the material of the indenter and that of the scratched material. The indenter scratches the surface of the sample in a straight line, traversing areas of matrix and fibre. The depth of the indenter is also recorded, thus indicating the hardness of the surface being scratched. Two values of the normal force were applied in the experiments in order to obtain more detail about the influence of the tip to the scratch morphology. Each matrix/fibre system was scratched with constant values of 1 and 0.4 mN normal force of the tip. The experiment was repeated several times for each system. The scratch length was about 60 μm starting from the matrix and crossing two fibres in this range that were found on the surface of each sample. Hence, two matrix/fibre interphase regions were investigated in one run. (The part of the scratch path from the fibre to the matrix could not be analysed due to the loss of balance in the system when the tip suddenly drops to softer material).

3. Experimental results

3.1. Indentation results

The load-displacement curves for each indent were recorded automatically in separate computer files. A typical load-displacement graph for indents in matrix, interphase and glass are shown in Fig. 3. Each curve consists of the loading portion (starting from the origin) and the unloading part (of steeper gradient). The indent in glass shows a better elastic recovery due to higher modulus of elasticity. The initial gradient of the unloading curve is used to calculate the stiffness of the sample at that point, as shown in the equation below:

$$S = \frac{\mathrm{d}P}{\mathrm{d}h} \tag{2}$$

where h is the depth of penetration as shown in Fig.1, and P the measured load. The stiffness is then used to obtain the reduced elastic modulus [15]:

$$E_r = \frac{\sqrt{\pi}}{2\beta}\frac{S}{\sqrt{A}} \tag{3}$$

where A is the contact area ($A = 24.5h_c^2$) and $\beta = 1.034$ for a triangular indenter [14]. The modulus of the indented material is now obtained from the following equation:

$$E_r = \left(\frac{1-\nu_i^2}{E_i} + \frac{1-\nu_s^2}{E_s}\right)^{-1} \tag{4}$$

where E_i, ν_i are the elastic modulus and Poisson's ratio of the indenter tip (diamond) and E_s, ν_s are the equivalent properties of the indented material. The modulus of elasticity for each indent is calculated with Poisson's ratio of the material obtained from the technical literature. The chosen Poisson's ratios, and the calculated elastic moduli for matrix, interphase and glass, are presented in Table 1.

Hardness values calculated using Eq. (1) for polyester/glass, CL1916/glass and CL1880/glass systems are shown in Fig. 4(a)–(c). The hardness values range from approximately 10 GPa for the glass to less than 1 GPa in the matrix. The transition region observed between the matrix and the fibre has a similar character for the polyester and the phenolic systems. This region shows material properties distinct from those of the matrix and the fibre. The width of the transition zone is approximately 1 μm.

3.2. Nano-scratch results

A typical scratch recording, including the profile depth

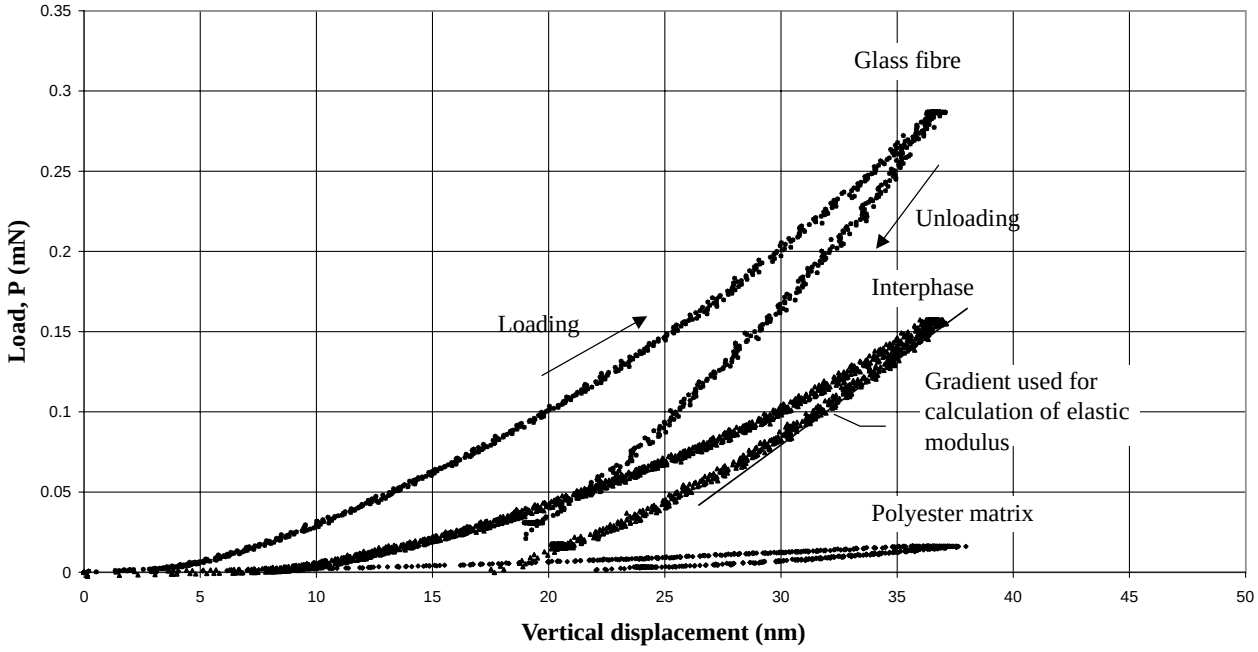

Fig. 3. A typical recording of load versus displacement during indentation test.

and the coefficient of friction is shown in Fig. 5. The profile depth is the penetrating depth of the tip in the material, influenced by the hardness of the scratched material. The coefficient of friction is determined from the ratio of the lateral and the normal force. Therefore, the coefficient of friction indicates the resistance of the material to the tip penetration in the tangential direction.

It is apparent that the width of the transition zone is equal to the distance B–H. Point B is defined as the departure of the profile depth from the horizontal slope *a*, and point H by the intersection of horizontal line *e* with the slanting line *d*. To the right of B, the indenter is entirely in the matrix whereas at H and to the left of H the indenter leading edge reaches the edge of the fibre and moves over the glass surface. The reasons for choosing points B and H are explained later.

Only the results for the polyester/glass system are presented here. The graphs for the other two systems are very similar (almost identical) and therefore not shown.

The apparent width of the transition zone is approximately 3.5 μm, which is much larger than that found in the indentation tests, due to the different test method. It is clear that this method provides more interesting details, revealed especially by the variation in the coefficient of friction, with a hump at point G. This has been observed practically in all measurements and therefore is thought to be a genuine effect associated with the movement of the indenter crossing the material interfaces, as discussed below.

4. Discussion

All the experimental results show a transition zone in the properties between the matrix and the fibre. We postulate that the transition zone effect is created by:

1. presence of an interphase of varying material properties;
2. interaction of the created stress field and plastic zone with the material interfaces;
3. finite width of the indenter and it geometry;
4. a combination of any of the above.

4.1. Interphase

There is a possibility for the formation of an interphase in our composite systems during the initial contact of the

Table 1
The elastic moduli calculated from the nano-indentation hardness results, for the glass fibre, glass–polymer interphase and the polymer matrix in three composite systems

E (GPa)	Glass	Interphase	Matrix	Poisson's ratio
Polyester/glass sample	95	52	6	0.38/0.22
Phenolic CL1916/glass sample	100	60	7	0.38/0.22
Phenolic CL1880/glass sample	90	50	7	0.38/0.22

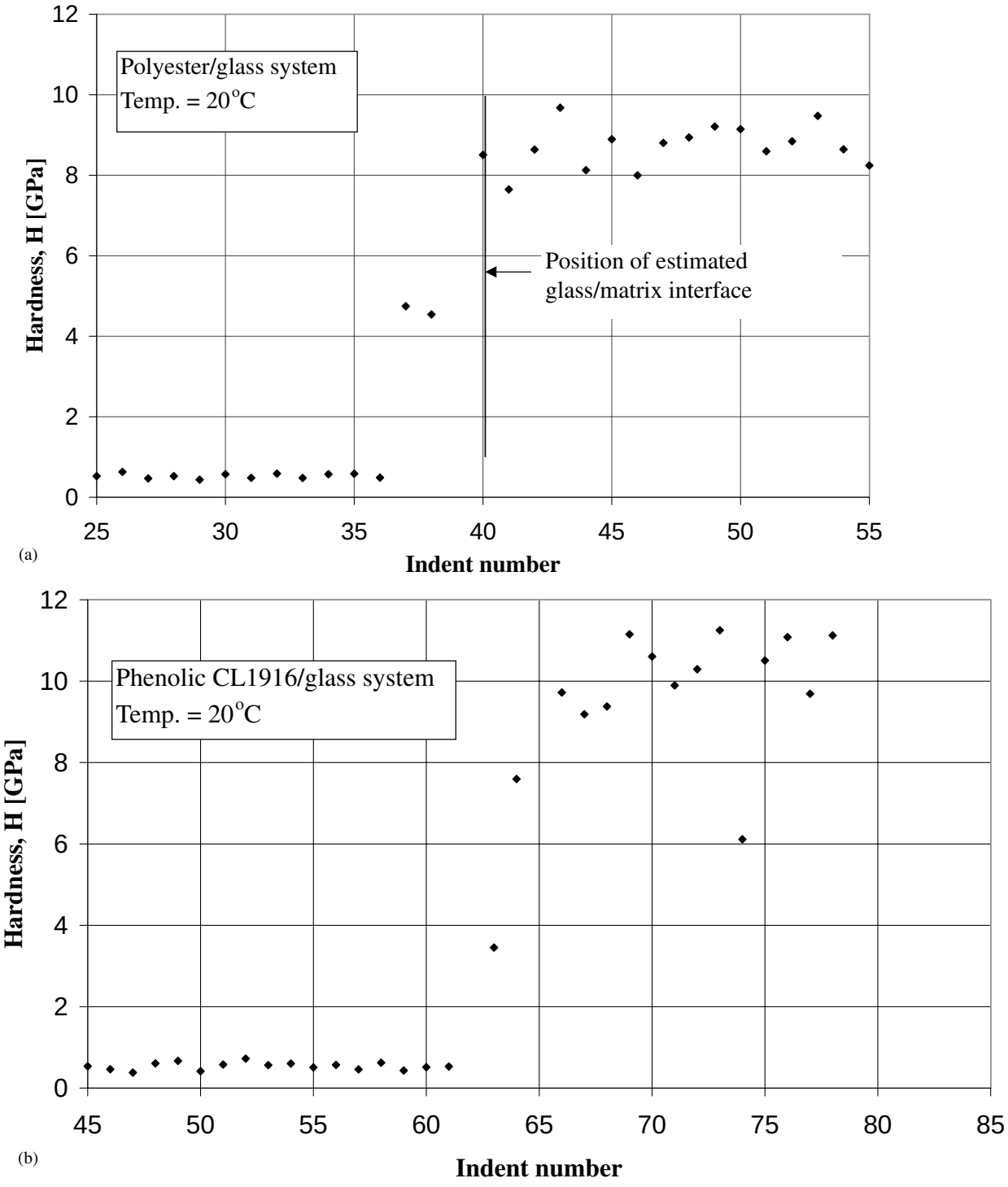

Fig. 4. Hardness calculated according to Eq. (1). Note the transition zone from the matrix (on the left) to the glass fibre (on the right).

curing resin with the silane coated glass fibres. Before cross-linking is completed, the liquid contains a mixture of polymers and oligomers, and therefore can be considered as a polymer blend [16]. During this stage, interdiffusion may occur leading to the formation of an interphase, as shown schematically in Fig. 6. This effect has been observed previously, and interphase widths of as much as 100 μm have been estimated for the case when there was excess of silane agent on the glass fibre surface [17].

Since the formation of such a layer is by the process of interdiffusion, a gradual variation of properties from pure matrix to pure silane should be expected. The friction or hardness properties of silanes are not known, therefore

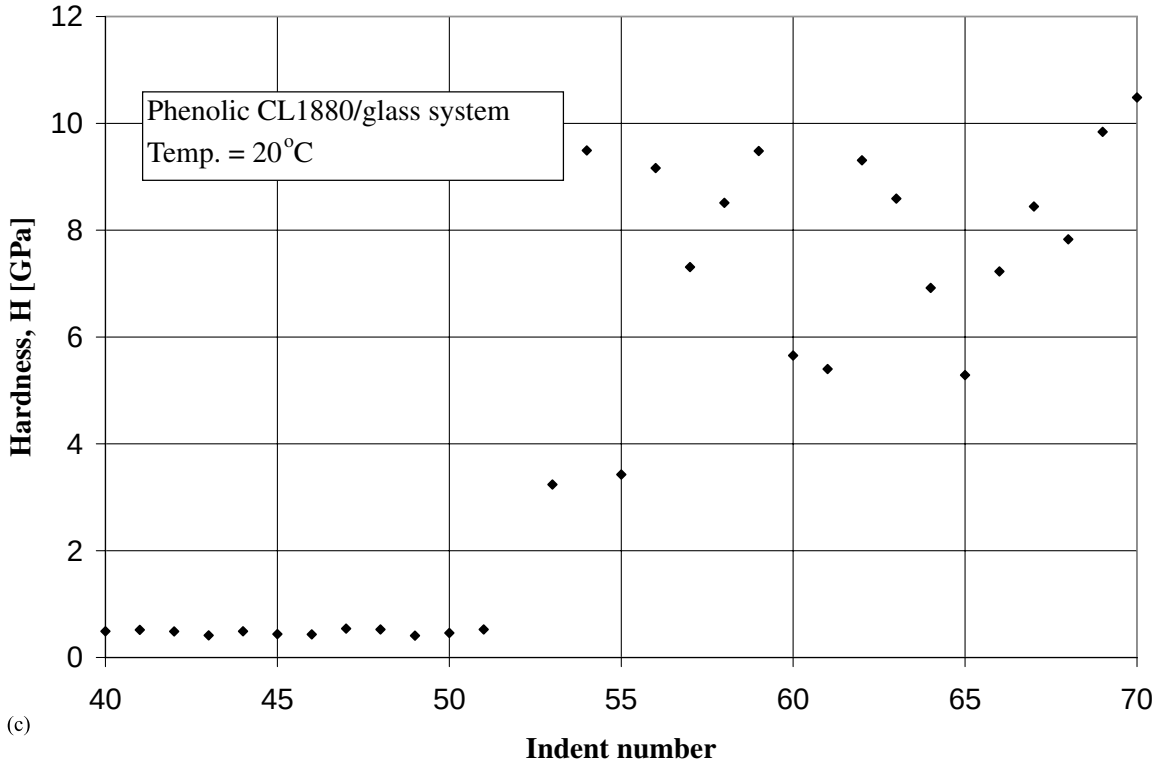

(c)

Fig. 4. (*continued*)

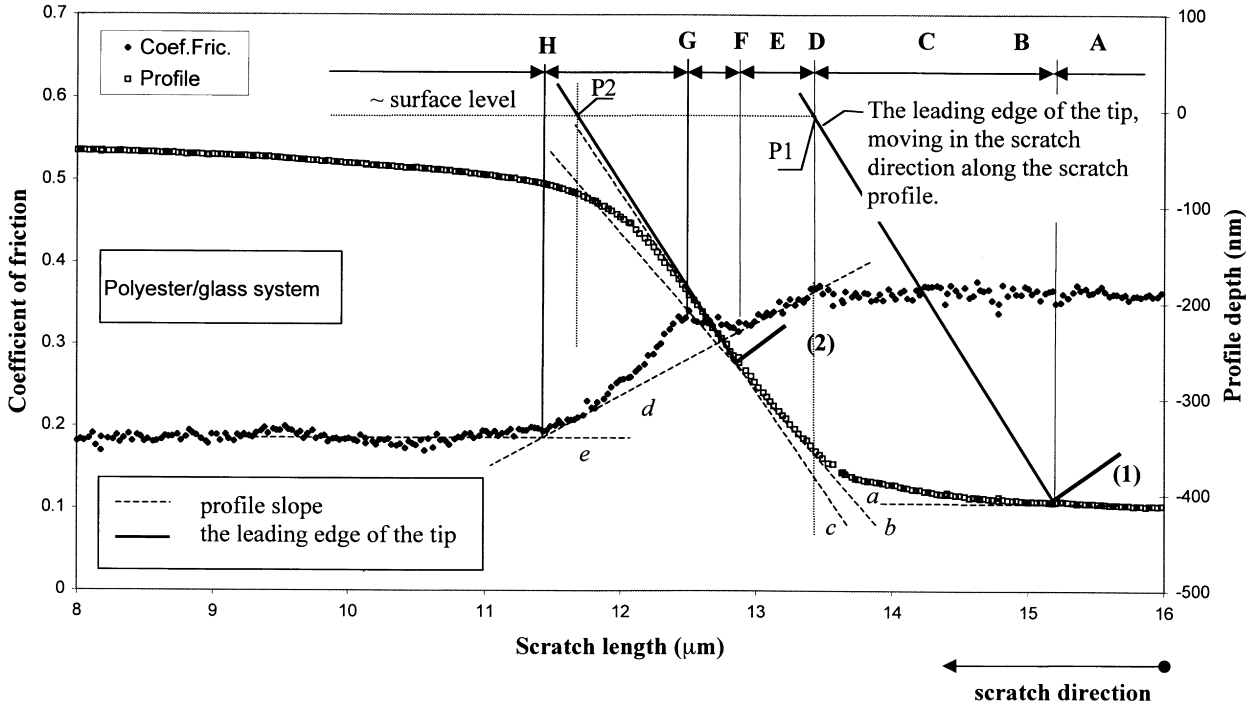

Fig. 5. A typical scratch recording for polyester/glass, including the profile depth and the coefficient of friction.

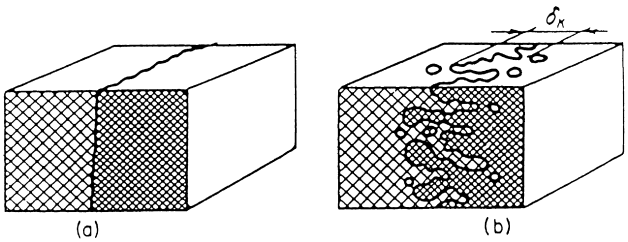

Fig. 6. Sharp and diffuse interface in a mixture of two components [16]. (a) Sharp interface between matrix and fibre coating. (b) Interphase created by interdiffusion of fibre coating and matrix.

quantitative evaluation of an interphase in our systems is not possible at this stage.

4.2. Stress field and plastic zone

When an indenter is pressed into the material it creates a corresponding stress field and associated zone of plastic deformation [18,19]. A schematic drawing of the plastic zone, of width W_{pl}, under a "frictionless" indenter is shown in Fig. 7. The stress field, and the creation of a plastic zone are affected by the presence of: (i) interfaces (as in matrix/glass); (ii) inclusions (i.e. filler or toughening particles); or (iii) an interphase with material properties distinct from those of the matrix. In our case we have (i), we presume the existence of (iii), and therefore an interaction effect should be expected.

The polyester and phenolic thermosetting polymers are materials for which the coefficient of work hardening is very small. Moreover, their elastic moduli are at least an order of magnitude less than that of glass. Therefore, in the case of these composite systems the stress and plasticity interaction effect should be negligibly small in the regions away from the matrix/glass interface. This is observed in the nano-indentation results (Fig. 4(a)–(c)). However, in close proximity to the interface with glass, the constriction on the development of the plastic zone should be evident as an increased resistance to indentation. This can be seen in Fig. 4 as points with hardness around 4 GPa. Such an increase in hardness above that of the matrix cannot possibly be due to the interphase alone (polyester–silanes mixture). From this we infer that the plastic zone width, W_{pl}, is approximately equal to twice the maximum width of the indentation.

4.3. Indenter width and geometry

The influence of different material regions in the sample on the tip behaviour and the scratch morphology are presented in Fig. 8(a)–(c). We define: W_{int} as the interphase width, and W_{tip} as the penetrating width of the tip. There are three possible cases:

1. $W_{int} > W_{tip}$;
2. $W_{int} \leq W_{tip}$,
3. $W_{int} = 0$.

4.3.1. The case when $W_{int} > W_{tip}$ (Fig. 8(a))

The penetrating depth of the scratch indicates the position of the tip. The scratch path and the penetrating depth of the tip are influenced by the contact of the tip's leading edge with the material at the surface of the sample. The information that is obtained from the tip is therefore delayed, and we have to take the influence of the tip's geometry into consideration. In Fig. 5 where the leading edge and the tip of the indenter are superimposed onto the graph of experimental results.

The transition zone is contacted first by the leading edge of the tip when the tip is at (B) position. At the same time, the edge of the indenter crossed the surface of the sample at point P1, already within the interphase region. This region, apparently harder than the matrix, forced the tip to lower penetrating depth while the tip moved through region (C). The projection of P1 onto the profile depth shows where the tip contacted the interphase region after being pushed up by

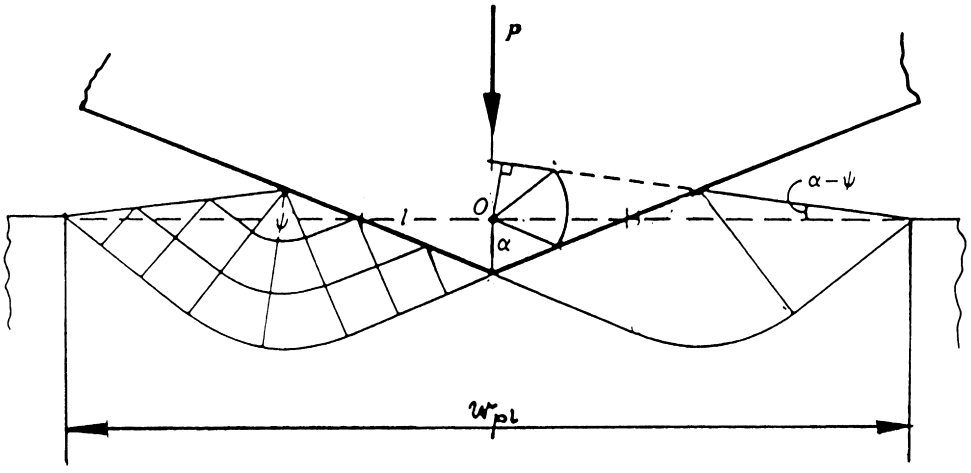

Fig. 7. Plastic deformation zone, of width W_{pl}, created by an indenter pressing into a ductile material (frictionless case, [18]).

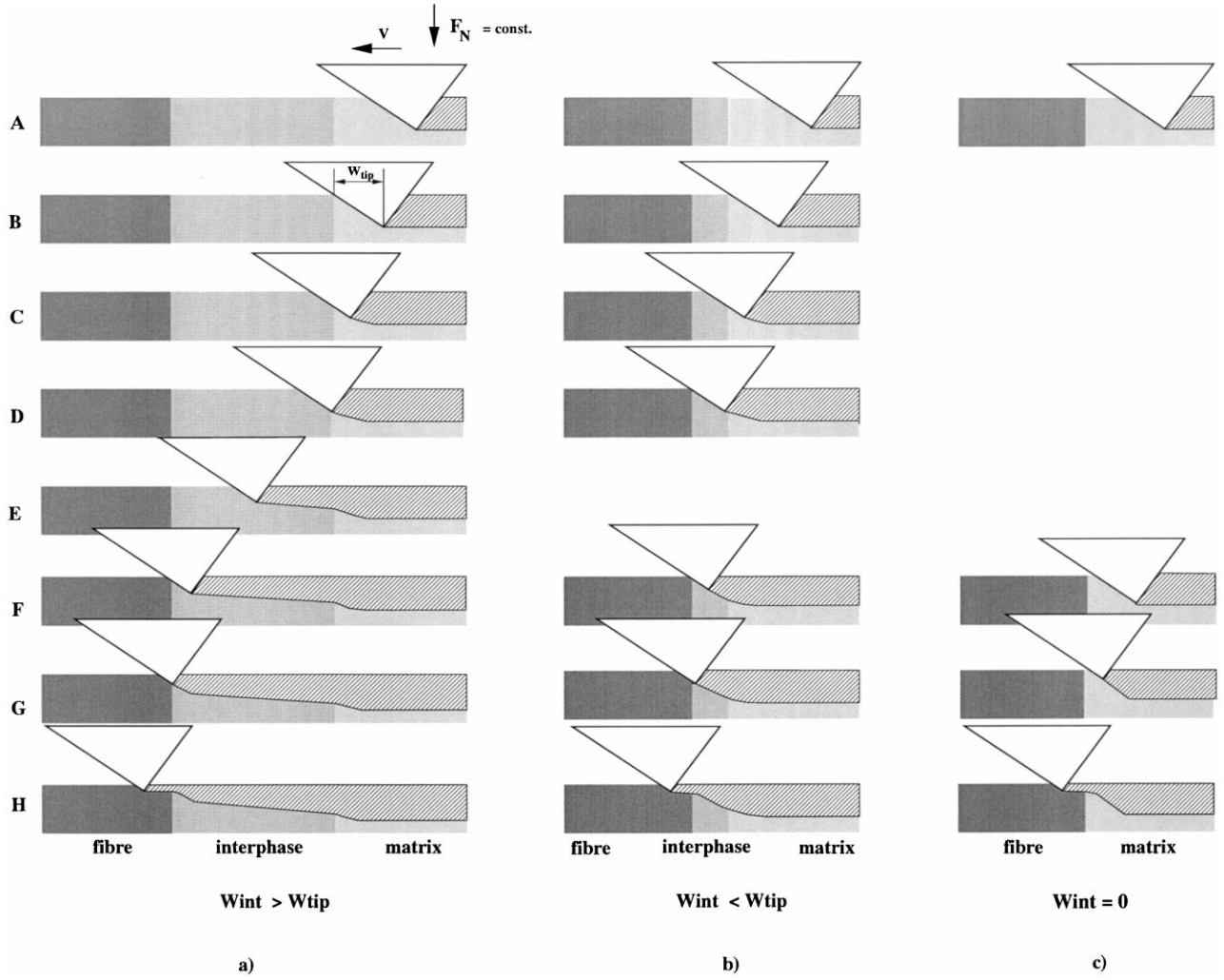

Fig. 8. Morphology of the scratch path for the three possible cases: the interphase width (a) greater or (b) lesser than the effective width of the indenter tip, and (c) equals zero (i.e. the sharp interface region).

its leading edge. However, that information could not reflect the genuine character of the interphase, as the edge of the tip already contacted the more harder region.

Once the indenter is fully in contact with the interphase zone (D), the gradient of the scratch path must change. In this stage, if the interphase region were to have constant material properties, the tip would move parallel to the surface. If the interphase properties exhibit a gradual change along its length, the tip will move correspondingly to a lower depth.

We note that the coefficient of friction gradually decreased after the tip reached the material at (D). This indicates a change in the material properties. The tip moved up toward the surface and the coefficient of friction decreased, indicating a region of material harder than that of the matrix. The slope of this profile path is denoted as *b*.

At stage (F), this trend is changed due to the sudden increase in the coefficient of friction, and the profile path follows a sharper slope *c*. Since the slope *c* is parallel to the leading edge of the tip, it is clear that the edge slid over the edge of the glass fibre, in order to maintain the constant normal force. The coefficient of friction at (F) has stopped decreasing due to the contact resistance of the tip at the glass fibre. Since the movement of the sample at this stage was limited to sliding of the tip over the fibre, the horizontal displacement of the sample was shorter than that in the previous stages. The complex interactions between the sample, the instrument and the tip resulted in the artificial increase in the coefficient of friction above that of line *d*, which only indicates the presence of the very hard forthcoming material, without information of the true character of the interphase in this region (F–G). The important parameter is the slope *c*. If the fibre had not been surrounded by the interphase region, the slope *c* would have appeared from the very start (Fig. 8(c)). The presence of the slope *b* proves that the edge of the tip contacted harder material that was not the glass fibre. This was later confirmed by the artificial increase in the coefficient of friction and the slope *c*, that could only be the consequence of the contact with the fibre.

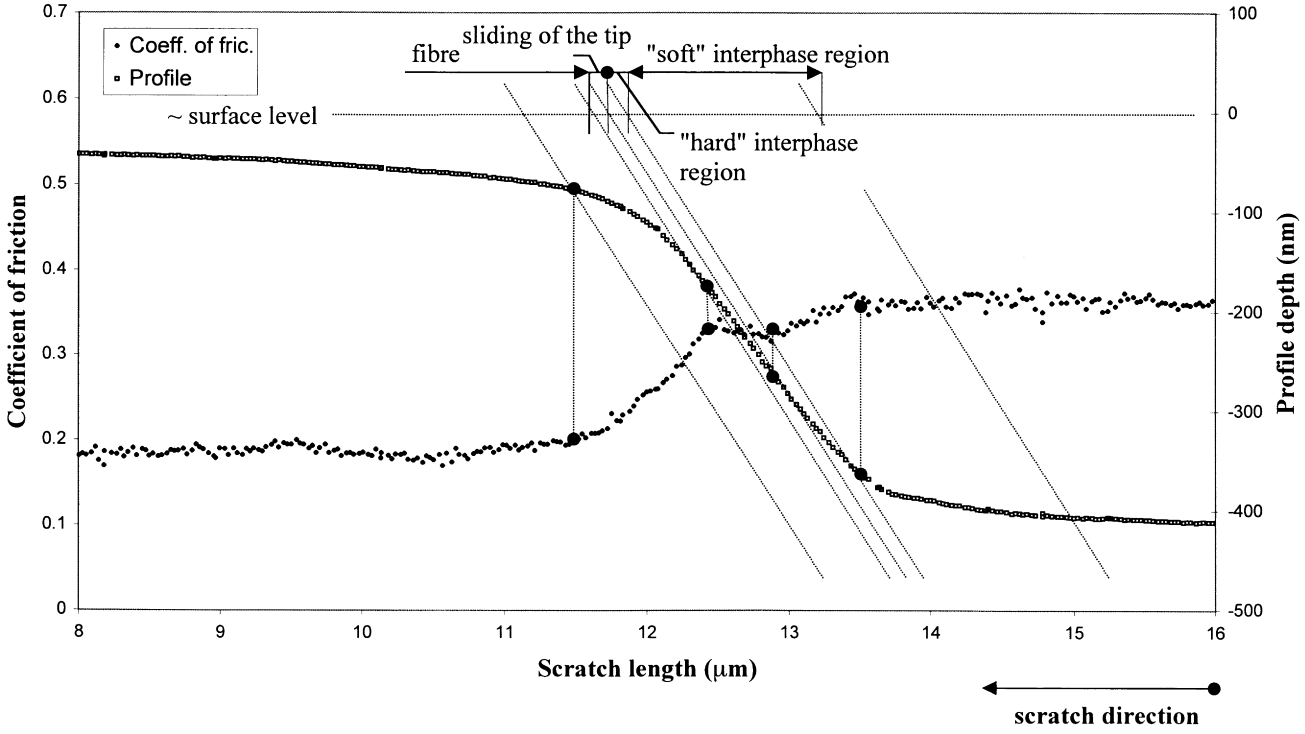

Fig. 9. The actual lengths of the characteristic parts of the scratch path, measured between the characteristic positions of the leading edge of the indenter.

In addition, the edge of the tip at stage (F) crossed the surface of the sample at point P2. The projection of this contact point onto the profile depth shows that this point of contact is the very start of the fibre, as explained in more detail below.

The region (G–H) shown in Fig. 5 is the transition region between the sliding path of the tip (F–G) and the actual fibre (H). At this stage, the tip gradually reached the appropriate depth in the fibre (it is possible that the edge of the diamond tip carved a shallow notch in the edge of the fibre, thus smoothing the path along the fibre's edge). The coefficient of friction steadily decreased in this region, both from the gradual change in the material properties and the contact between the fibre and the edge of the tip.

(H) denotes a path in pure fibre, starting from the point where the tip fully contacted the fibre after the (G–H) region. This is also found from the point where the coefficient of friction reaches a constant value. The slope *d* joins the start and the end of the decreasing trend in the coefficient of friction, while the slope *e* represents the trend of the constant value in the fibre. The crossing point of these two slopes indicates the point where the tip reached the full contact with the fibre (H).

The actual lengths of the characteristic parts of the scratch path are shown in Fig. 9. The test results, i.e. the profile depth and the coefficient of friction, include both, the motion of the tip, and the scratch path. In order to get the scratch path only, the lines parallel to the edge of the tip are drawn at the characteristic points of the scratch graph. These lines represent different positions of the edge of the tip, placed at the points where different material properties were detected along the scratch, as in Fig. 5. Relative positions between these lines represent genuine lengths of the scratch stages in the scratch direction, excluding the vertical displacement. The already determined interphase region comprises the "soft" (closer to the matrix) and the "hard" (closer to the fibre) regions, parts of the same exponential function (B–F). The determined widths of the interphase regions, derived from the nano scratch test, are shown in Fig. 10. The results of the tests with two different applied normal forces were consistent.

4.3.2. Analysis of the scratch path when $W_{int} < W_{tip}$ (Fig. 8(b))

The case when the interphase width is lesser than the penetration width of the tip's leading edge is shown in Fig. 8(b). In this case, some stages are missing, as the tip's leading edge comes into contact with the fibre's edge before the interphase region is contacted by the tip. Therefore, although it is possible to detect the start of the interphase region, the information about the character of the interphase is obscured by the influence of the harder fibre. In this case, if the surface level is unknown, it is convenient to measure the interphase width as between the leading edge positions at (B) and (D).

4.3.3. Analysis of the scratch path when $W_{int} = 0$ (Fig. 8(c))

The third possible case is the sharp interface between the fibre and the matrix. Even if $W_{\mathrm{int}} = 0$, there will be a transition zone >0 because of the finite width of indenter and

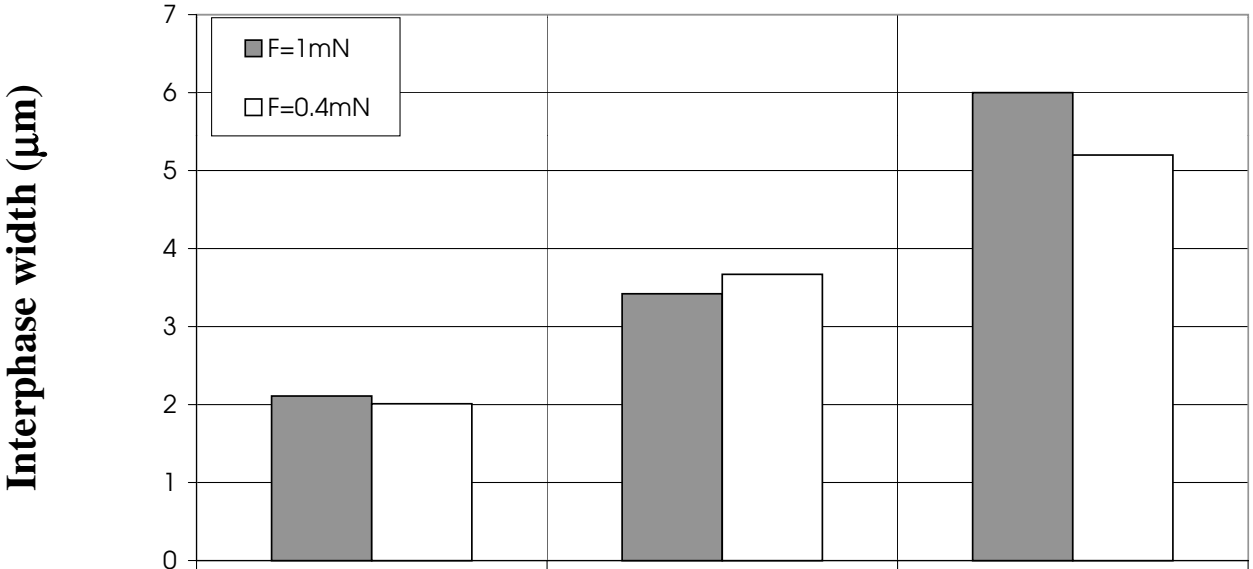

Fig. 10. The determined widths of the interphase regions, investigated by the nano scratch test, for the three polymer/glass systems and two values of the normal force. The consistency of the results is striking.

because of the stress field and plastic zone interaction with glass/matrix interface. After the fibre is contacted by the edge of the tip, the tip slides over the fibre's edge in order to maintain the constant normal force. At this stage, the tip is unable to produce a scratch due to the strong contact resistance from the glass fibre. The tip slides to a lower depth with the contact resistance subsequently decreasing until an appropriate depth is reached, enabling the tip to move gradually in the scratch direction. In other words, the scratch path over the sharp interface includes three characteristic stages: the sharp slope parallel to the leading edge of the tip (F), gradually decreases to a lower gradient slope (G), finally reaching the horizontal scratch path in the fibre (H).

4.4. Surface preparation

For further development of this technique, greater attention must be paid to the preparation of the test surfaces. In our final polishing stage, alumina paste of 50 nm particle size was used. This must be viewed in terms of the indentation depths of 30 nm. It would be reasonable to assume that the scatter in our data, of the order of 20%, is partly due to the insufficient smoothness of the surfaces. The other question to be considered is whether indentations in polymeric materials to a depth of 30 nm can be considered as the representing the bulk of the material. One can expect that gasses, water vapour and other elements, adsorbed on the surface, will diffuse in very likely to the depth of 5–10 nm, thus affecting the properties of the polymers. By contrast, the scratch test, which is in load control mode, reaches depths ten times as great in the polymer phase, thus sampling a much larger volume and therefore being more reliable.

5. Conclusions

It was shown that the nano indentation and the nano scratch test could be successfully employed in the investigation of composite interphases. The interphase region in composite materials has been in focus of several destructive and non-destructive experimental techniques over the last two decades. The results have shown similar trends, however, the detected width of the interphase region varied depending on the character of the experiment. The nano-indentation has proved to be a reliable experimental technique in this direction, in conjunction with the nano scratch test. The width of the interphase region between the fibre and the matrix was detected by both techniques. The results were consistent although materials had different surface morphologies, with phenolics being more inhomogeneous than polyester. The nano-indentation test detected material properties of different constituents in composite systems, including the stronger material properties of the interphase region than the matrix in each material. These results were confirmed by the strong change in the coefficient of friction along the interphase region in the nano-scratch test.

The mechanical analysis of the indentation test showed that the region in material affected by the indentation of a pyramidal tip was of a much lesser order than the width

detected in the experimental part. Therefore, the results in the interphase region could not be merely influenced by the presence of the fibre, as the experimentally detected interphase width exceeds the region of the fibre's influence. The scratch test appears to be a more sensitive technique for detecting interphases than the indentation technique.

Acknowledgements

The authors from the Australian National University would like to thank the Aeronautical and Maritime Research Laboratories, Melbourne, Australia, and in particular, Dr Adrian Mouritz for their support and guidance. The first author would like to thank Dr Adrian Lowe for initiating the contact with the Hong Kong University of Science and Technology and Dr J.K. Kim for financial support. The nano-indentation and the nano-scratch tests were conducted with the technical support of Advanced Engineering Materials Facilities (AEMF) at the Hong Kong University of Science and Technology.

References

[1] Kim JK, Mai YW. Engineered interfaces in fiber reinforced composites. New York: Elsevier, 1998 (chap 7).
[2] Plueddemann EP. Silylated surfaces, London: Gordon and Breach, 1980. p. 31–53.
[3] Drown EK, Al-Moussawi H, Drzal LT. J Adhes Sci Technol 1991;5:865–81.
[4] Drzal LT, Herrera-Franco PJ. Engineered materials handbook, vol 3. ASM International, 1991. p. 391–405.
[5] Young RJ, Huang YL, Gu X, Day RJ. Plast. Rubber Compos Process Appl 1995;23:11–9.
[6] Robinson IM, Zakikhani M, Day RJ, Young RJ, Galiotis C. J Mater Sci Lett 1987;6:1212–4.
[7] Ishida H, Koenig JL. J Colloid Interface Sci 1978;64:555–64.
[8] Ishida H, Koenig JL. J Polym Sci, Part B Polym Phys Ed 1979;17:615–26.
[9] Hoh KP, Ishida H, Koenig JL. Polym Composites 1988;9:151–7.
[10] Hodzic A, Kalyanasundaram S, Lowe AE, Stachurski ZH. Composite Interfaces 1999;6(4):375–89.
[11] Wang HF, Nelson JC, Gerberich WW, Deve HE. Acta Metall Mater 1994;42(3):695–700.
[12] Steinmann PA, Tardy Y, Hintermann HE. Thin Solid Films 1987;154:333–49.
[13] Sham ML, Kim JK, Wu JS. Submitted for publication, 1999.
[14] Bharat Bhushan. Handbook of micro/nanotribology. Boca Raton: CRC Press, 1995 (chap 9).
[15] Nano Indenter II Operating Instructions. Nano Instruments Inc., P.O. Box 14211, Knoxville, TN 37914., 1995. p. 321–96.
[16] Utracki LA. Polymer alloys and blends. Munich: Hanser, 1989.
[17] Ikuta N, Suzuki Y, Maekawa Z, Hamada H. Polymer 1993;36:2445.
[18] Johnston KL. Contact mechanics. Cambridge: Cambridge University Press, 1987.
[19] Landan LD, Lifshitz EM. Theory of elasticity. Oxford: Pergamon Press, 1965.